Recording Density Limit of Photon-echo Optical Storage With High-speed Writing and Reading

Kröll, Stefan; Tidlund, P

Published in:
Optical Society of America. Journal B: Optical Physics

DOI:
10.1364/AO.32.007233

1993

Recording density limit of photon-echo optical storage with high-speed writing and reading

S. Kröll and P. Tidlund

The first analysis to our knowledge of the optical data storage density of photon-echo storage is presented. Mainly considering signal-to-noise ratio performance, we calculate the obtainable storage density for data storage and processing using photon echoes to be approximately 100 times the theoretical limit for conventional optical data storage. This limit is similar to that theoretically calculated for data storage by use of persistent spectral hole burning. For storage times longer than the upper-state lifetime the highest densities can, however, be obtained only if all the excited atoms decay, or are transferred, to a different state than that from which they were originally excited. The analysis is restricted to samples with low optical density, and it also assumes that for every data sequence, writing is performed only once. It is therefore not directly applicable to accumulated photon echoes. A significant feature of photon-echo storage and processing is its speed; e.g., addressing 1 kbyte/(spatial point) permits terahertz read and write speeds for transitions with transition probabilities as low as 1000 s^{-1}.

1. Introduction

Time-domain optical data storage[1] and processing by use of photon echoes have received increasing attention during recent years.[2–8] A conceptual view of the technique is shown in Figure 1. A particularly attractive feature of time-domain and frequency-domain optical storage is the ability to store many bits of information in a diffraction-limited spot[9] and thereby increase the data storage density. In frequency-domain optical storage (FDOS) a large number of bits are stored at each spatial location by a change in the frequency of the light for each bit, while in time-domain optical storage (TDOS) with photon echoes, the temporal Fourier transform of the input data sequence from a light source emitting at a fixed frequency is written into the inhomogeneous absorption profile. To store and to recall the input data faithfully, the Fourier transform of the input data sequence must therefore be narrower than the inhomogeneous linewidth. This requirement on the Fourier transform of the input data sequence sets an upper limit for the TDOS read–write data rate that essentially equals the inhomogeneous bandwidth of the transition. For FDOS the maximum data rate instead equals the inhomogeneous linewidth divided by the number of bits stored in each spot. The effect of this is that for a typical storage material the theoretical value for the maximum write–read rate of TDOS exceeds that of FDOS by 10^2–10^6 (compare, e.g., Ref. 9). There have been two in-depth analyses of the storage density that can be obtained with the FDOS approach and the material requirements necessary to obtain these densities.[10,11] The material requirements and obtainable storage densities for TDOS may be different from those in FDOS, since the physical mechanism for storage is different for the two methods. Material requirements and theoretical limits for TDOS storage are therefore analyzed in this paper. Because of the high write–read rates for TDOS, some aspects of data processing with photon echoes are also considered. There are approaches to TDOS that are not covered in the present analysis, e.g., accumulated photon echoes, in which each data bit is written into the sample several times,[3–6] or hybrid techniques in which the spectral profile is divided into several sections. Addressing different sections is then done by scanning of the laser frequency, i.e., a FDOS approach, but within each section, data are addressed by use of photon echoes.[12,13] These alternative implementations of TDOS may be expected to be capable of higher storage densities, but on the other hand, they may be expected to have lower data rates. Photon echoes also have the unique property of retaining all phase information in the excitation pulses. This is an aspect of TDOS that still has not been investigated in much detail.

The authors are with the Department of Physics, Lund Institute of Technology, Box 118, Lund S-22100, Sweden.

Received 28 August 1992.
0003-6935/93/357233-10$06.00/0.

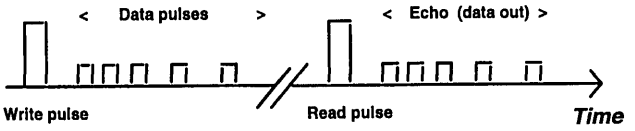

Fig. 1. Conceptual picture of time-domain optical storage and processing. The write pulse stores the temporal Fourier transform of the data input sequence in the material. The read pulse recalls the stored sequence. Each output data pulse is the correlation of the corresponding input data pulse and the write pulse convoluted with the read pulse.

Future data storage schemes not anticipated at this time may alter the capabilities of TDOS storage significantly. Implementations of TDOS not covered by the present analysis and the effect of these on the range of validity of the analysis are given in Table 1.[14,15]

2. Model

The most important quantities used in the calculations below are summarized and defined in Table 2 as a handy reference for the reader as the calculations develop. The range of validity for several of the quantities is also given in Table 2.

A. Number of Photons per Data Bit

The analysis is primarily based on signal-to-noise-ratio (SNR) considerations. An expression for the number of photons in a stimulated photon echo is therefore needed. Such an expression is now derived based on the description by Abella *et al.*[16] The photon echo is emitted from an ensemble of excited atoms that together have a macroscopic dipole moment. The number of photons S_e emitted from such a superradiant state during a time t is approximately

$$S_e = \frac{N_e^2 p(t)}{4}. \tag{1}$$

Table 1. Limitations of the Analysis

Assumptions	Methods Not Covered	Comments
Single-shot read and write.	Accumulated photon echoes[3–6] and hybrid techniques.[12,13]	These methods would have higher storage capacities at the expense of slower data rates.
Stored information is intensity coded.	Phase-coded information storage[14,15] and methods that use external fields.[a]	Photon-echo storage is unique in the way it preserves the phase information of the stored information. This is still a largely unexplored area.

[a]See the Note added in proof at the end of this paper.

N_e is the number of excited atoms, and $p(t)$ is the probability that any single atom will radiate during time t.[16,17]

Consider a material doped with active centers of some concentration n, which has a transition with an inhomogeneous linewidth $1/(\pi T)$, where T is the inhomogeneous relaxation time. Assuming the laser linewidth is Fourier limited, the number of centers in a sample of length L, excited by a laser pulse of cross-sectional area A_x and duration τ, is

$$N_e = \alpha n A_x L \frac{T}{\tau}. \tag{2}$$

T/τ is the fraction of centers within the inhomogeneous linewidth excited by the pulse of duration τ, and α depends on the pulse area of the excitation pulse ($\alpha \leq 1$). The probability that any single atom makes a transition by spontaneously emitting a photon during the time τ is $A\tau$, where A is the transition probability. For optimum pulse area $\alpha = 1$ the number of photons emitted in a two-pulse photon echo (S_{2-p}) can then be written[16] as

$$S_{2-p} = \left(\frac{n}{2} A_x L \frac{T}{\tau}\right)^2 A\tau \left(\frac{3\lambda}{8L\sqrt{\epsilon}}\right). \tag{3}$$

The factor $3\lambda/(\triangle((8L\sqrt{\epsilon})$ arises when the photon-echo signal is integrated over all angles of propagation [assuming $A_x \ll 4\lambda L$ (Ref. 16, App. C)]. λ is the transition wavelength, and $\sqrt{\epsilon}$ is the index of refraction at this wavelength.

We now wish to modify this expression such that it expresses the number of photons in a stored data bit that is recalled by a stimulated photon echo. The write and the data pulses perform the task of storing the Fourier transform of the data sequence as a frequency-dependent modulation of the upper- and lower-state populations within the inhomogeneous profile.[9] When the upper-state population decays, there is a certain probability η for each atom not to return to its original state. When the upper state has decayed, there is therefore a remaining frequency-dependent modulation in the lower state that essentially equals the modulation before the upper-state relaxation, multiplied with the factor η ($\eta < 1$). The read pulse then transfers the lower-state atoms to the excited state, and a fraction η of the excited atoms then forms the superradiant macroscopic state reradiating the previously stored data sequence. Because the number of excited atoms emitting the echo equals the number excited after the first two pulses multiplied by a factor η, the number of photons S in the stimulated echo is

$$S = S_{2-p}\eta^2 \sin^2\theta_w \sin^2\theta_d \sin^2\theta_r. \tag{4}$$

θ represents the pulse areas of write, data, and read pulses (compare, e.g., Ref. 18). Our analysis primar-

Table 2. Definition of Variables

Symbol	Quantity	Comment
N	Number of bits stored at each spatial location.	
A	Einstein coefficient of the transition.	
τ	Duration of one data bit.	
η	Probability that an atom excited by a data pulse will store information.	The analysis shows that the material parameters predominantly determining the obtainable storage capacity are η and the product $NA\tau$.
λ	Wavelength of the excitation light.	In the calculations, $\lambda = 600$ nm.
k	$A_x = (k\lambda)^2$.	A_x is the area in which the N data bits are stored.
N/k^2	Fractional increase in storage density in comparison with conventional optical storage.	It is assumed that conventional optical storage is capable of storing 1 bit/λ^2.
L	Length of storage volume ($L = 2A_x/\lambda$).	For consistency with previous investigations[10,11] the length is chosen in terms of the Rayleigh length of the focused laser beam.
S	Number of photons in the detected signal ($S = 400$)	This value certifies that the required SNR is the same (20 dB) as in Refs. 10 and 11.
n	Density of centers that may store information.	
n_{max}	Maximum density of centers for storing information ($n_{max} = 10^{26}/m^3$)	Higher concentrations are assumed to lead to too large an interaction between the active centers. The present value is already a bit high for larger molecules, but when the active center is an atomic ion or a small molecule, this concentration is feasible.
$n\sigma L$	The sample transmission is $\exp(-n\sigma L)$. The maximum value of $n\sigma L$ in this paper is $(n\sigma L)_{max} = 0.3$, which corresponds to 25% absorption.	The reason for this upper limit is that the analysis is made assuming an optically thin sample. Higher absorption is expected to yield somewhat higher storage density. But the limit used here is expected to give results of the correct order of magnitude.
T_2	Homogeneous dephasing time.	
T	Inhomogeneous dephasing time.	
I_{th}	Maximum light intensity that can be applied without increasing the sample temperature.	Chosen to be 10^4 W/cm^2 for crystalline materials submerged in superfluid liquid helium.[10]
η_0	Probability the reading process will destroy the stored information.	Assumed to be zero when the equations are displayed in the figures.
m	Number of times a stored bit of data is read.	
ξ	Detector quantum efficiency.	In the calculations, $\xi = 0.75$.
ϵ	Index of refraction squared.	In the calculations, $\epsilon = 2.25$.

ily explores the SNR limits of photon-echo storage and processing, as previously noted. To maximize the SNR, we assume henceforth that read and write pulse areas are chosen such that the number of signal photons is maximized; i.e., $\theta_w = \theta_r = \pi/2$. The pulse area for each individual data pulse θ_d is chosen such that

$$\theta_d = \pi/(2N). \tag{5}$$

N is the number of bits addressed in each spatial point. This is the largest area that can be selected because a total data pulse area θ (whole data sequence) $= N\theta_d > \pi/2$ is expected to destroy the fidelity of the data reconstruction.[19]

To limit the diameter of the focused read and write beam at the sample edges, we chose the sample length to be twice the Rayleigh length,

$$L = 2A_x/\lambda. \tag{6}$$

Further, the area of the laser focal spot is rewritten as

$$A_x = (k\lambda)^2. \tag{7}$$

For $k = 1$, A_x (approximately) corresponds to the smallest area to which a laser beam can be focused. From Eqs. (1)–(7) we can express the number of photons detected for each single data bit as

$$S = \frac{3\pi^2}{64}\frac{\xi}{\sqrt{\epsilon}} n^2 k^6 \lambda^6 \eta^2 \frac{T^2}{N^2}\frac{A}{\tau}. \tag{8}$$

ξ is the detector quantum efficiency, and $\sin\theta_d$ is approximated by $\pi/(2N)$.

B. Signal-to-Noise-Ratio Limit of High-Density Time-Domain Optical Storage

An interesting parameter from a data-storage-density point of view is N/k^2. This is an expression for the storage density when N bits are stored in each spatial point of area A_x by use of TDOS, which is divided by the maximum storage density theoretically obtainable with conventional optical storage at the same wavelength. Thus N/k^2 is the fractional increase in storage density obtainable with photon-echo storage instead of conventional optical storage. Equation (8) can then be rewritten as an upper limit of the fractional increase in storage density:

$$\frac{N}{k^2} < \frac{\pi}{8}\left(\frac{3\xi}{\sqrt{\epsilon}}\right)^{1/2} nk\lambda^3\eta\,\frac{T}{\tau}\left(\frac{A\tau}{S}\right)^{1/2}. \tag{9}$$

Inequality (9) is used as a starting point for showing that any material capable of a fractional storage-density increase of N/k^2 with TDOS is constrained to a given region in a space spanned by the two parameters $NA\tau$ and η. Other particularly relevant material parameters in inequality (9) are the density of active centers, n, and the inhomogeneous relaxation time, T. According to inequality (9), the higher the value of T, the higher is the storage density that can be obtained. Thus to obtain as high a storage density as possible, T in inequality (9) is set equal to τ, which corresponds to utilization of the full inhomogeneous bandwidth of the storage material (if $T > \tau$, the Fourier transform of the data sequence exceeds the inhomogeneous bandwidth of the transition, and the data sequence cannot be faithfully reproduced). For $T = \tau$, inequality (9) can be rewritten as a lower limit on $NA\tau$ as a function of η for any given value on N/k^2, yielding

$$NA\tau > \frac{64}{3\pi^2}\frac{\sqrt{\epsilon}}{\xi}\frac{1}{n^2\lambda^6}\frac{1}{\eta^2}\left(\frac{N}{k^2}\right)^3 S. \tag{10}$$

Alternatively, using[20,21]

$$T = 4\left(\frac{\pi}{\ln 2}\right)^{1/2}\frac{1}{\lambda^2}\frac{\sigma}{A}, \tag{11}$$

where σ is the absorption cross section for the transition and $\lambda = L/(2k^2)$ from Eqs. (6) and (7), we can rewrite inequality (9) as

$$\frac{N}{k^2} < \frac{\pi}{4}\left(\frac{3\pi\xi}{\ln 2\sqrt{\epsilon}}\right)^{1/2}(n\sigma L)\frac{\eta}{k}\frac{1}{\sqrt{S}}\frac{1}{\sqrt{A\tau}}. \tag{12}$$

Inequality (12) can now be used to give an upper limit on $NA\tau$ versus η for any given value of N/k^2:

$$NA\tau < \frac{3\pi^3}{16\ln 2}\frac{\xi}{\sqrt{\epsilon}}\eta^2\frac{1}{S}\frac{(n\sigma L)^2}{(N/k^2)}. \tag{13}$$

Inequalities (10) and (13) now define the permissible area in $NA\tau$-versus-η space for the storage materials. Our purpose is first to find the largest area possible. The remaining material parameters are therefore chosen to maximize the permissible area. In inequality (10) the remaining material parameter is the concentration of the active center, n. To minimize the lower limit, we should use as high a value of n as possible. Too high a concentration of centers, however, promotes intercenter interaction that may destroy the stored information; compare Ref. 10. Here, a maximum concentration of $\sim 0.5\%$ is chosen as the upper limit, corresponding to $n_{\max} = 10^{26}/\mathrm{m}^3$. In inequality (13) the logarithm of the sample absorption $n\sigma L$ should be chosen to be large as possible to maximize the upper limit of $NA\tau$. However, our derivation of the number of photons in the photon-echo signal is valid only for optically thin samples. Thus we somewhat arbitrarily restrict the sample absorption to 25%, corresponding to $(n\sigma L)_{\max} = 0.3$. The only source of noise considered here is shot noise. For consistency with the previous analyses for FDOS[10,11] we need a SNR of 20 for TDOS; thus the minimum number of photons that must be detected is 400, i.e., $S = 400$. The remaining parameters, detector quantum efficiency, index of refraction, and wavelength, are chosen to be 0.75, 1.5, and 600 nm, respectively, which should facilitate comparisons with Refs. 10 and 11. The permissible material parameter space as limited by inequalities (10) and (13) is plotted in Fig. 2 for storage densities of 1, 10, and 100 times the limit for conventional optical storage at 600 nm. We see that the highest storage density that theoretically can be obtained is slightly greater than 100 times the conventional limit. At $\lambda = 600$ nm,

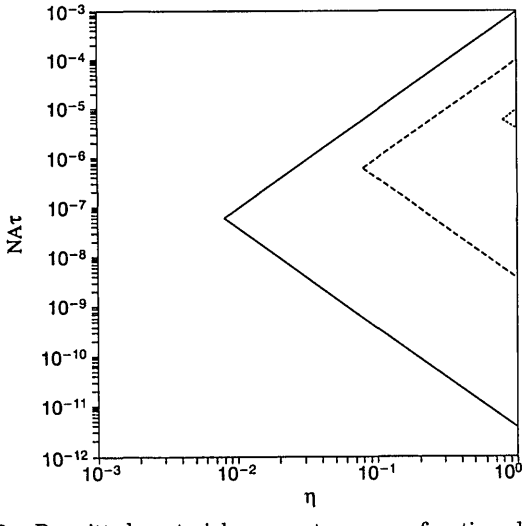

Fig. 2. Permitted material parameter space for time-domain optical storage for storage densities equal to 1, 10, and 100 (solid, long-dashed, and short-dashed curves, respectively) times the theoretical limit for conventional optical storage. The permitted area for each case is the triangle-shaped region to the right of the curve. η is the branching ratio; on the vertical axis N is the number of bits addressed in each spatial point, A is the transition probability, and τ is the duration of each data bit.

TDOS consequently should be capable of ~30 Gbits/cm^2.

C. Data Readout Process

So far we have not taken into account the fact that the reading process would generally tend to destroy the stored information. As an example, the case of rare-earth-ion-doped inorganic crystals is considered. The result and conclusions, however, should be applicable to most potential storage materials. For the rare-earth-ion-doped crystals primarily investigated to date for TDOS, data have been stored as a modulation of the population in the ground-state hyperfine levels. In these crystals, information may be destroyed both when the ground-state atoms are excited by the read pulse and when the ions excited by the read-pulse decay after emission of the stored data sequence. Information is stored in relaxation processes that reorient the rare-earth-ion nuclear spin with respect to the local field gradient at the ion site. The probability of reorienting the nuclear spin at direct optical excitation or de-excitation may be small; let us denote this probability η_0. Most of the excited ions will, however, decay through cascade processes involving several states. In this decay there is a probability for re-orienting the nuclear spin in each of the steps in the cascade process.[22] The total probability for changing the spin orientation during the decay process is then basically obtained by addition of the probabilities in all the individual steps. This total probability is the earlier-mentioned branching ratio η which is generally larger than η_0. The read pulse consequently destroys the population modulation with a probability η_0, and the relaxation process afterwards does the same with the probability η. Thus based on the above discussion, Eq. (8), which expresses the number of photons in a recalled data bit, can be rewritten to incorporate the effect of destructive reading. With replacement of η^2 by $\eta^2(1-\eta)^{2(m-1)}(1-\eta_0)^{2m}$ the number of photons contributing to the signal for read number m is

$$S = \frac{3\pi^2}{64}\frac{\xi}{\sqrt{\epsilon}} n^2 k^6 \lambda^6 \eta^2 \frac{T^2}{N^2}\frac{A}{\tau}(1-\eta_0)^{2m}(1-\eta)^{2(m-1)}. \tag{14}$$

Although the discussion above concerns rare-earth-ion-doped inorganic crystals specifically, the modification of Eq. (8) for including many reads in Eq. (14) should be more or less applicable to most potential storage systems. For many systems, η_0 is zero since the state at which the information-storing relaxation process (branching) occurs cannot be excited by the read pulses. η_0 can be expected to be small in many other systems also, and it is henceforth neglected. With replacement of η^2 in inequalities (10) and (13) by $\eta^2(1-\eta)^{2(m-1)}$ the permissible area for TDOS materials can also be plotted with the number of reads m as a parameter. In Fig. 3 the permissible area for TDOS storage with destructive reading is shown. The storage density is chosen to be equal to the theoretical limit of conventional optical storage. Data are assumed to be read 1, 5, and 25 times. For 50 consecutive destructive read pulses there is no permissible area. Further, for a storage density of ten times the conventional limit, only five consecutive destructive reads are possible before the permissible area shrinks to zero. These results clearly show that destructive reading is more or less impossible for a high-performance TDOS storage system. The equations and graphs in the remaining part of the paper are therefore valid either for so-called photon-gated storage[23,10] or for data-processing-type applications, which are assumed to be performed before the ions in the upper state have decayed. In photon-gated TDOS an extra laser pulse, normally at a wavelength different from that of the write, data, and read pulses, is applied after the write and data pulses (but before the read pulse). This pulse transfers the upper-state atoms to some reservoir state, thereby yielding a branching ratio η of, in the optimum case, unity. (Photon-gated storage has not been experimentally demonstrated for TDOS but the scheme suggested above should be a straightforward extension of photon-gated storage in FDOS.[23]) In the reading process the atoms transferred to the reservoir state then cannot be excited to the upper state, as a wavelength different from that of the read pulse would be needed. The branching ratio with no gating pulse should be very small, preferably zero. The stored information then cannot be destroyed in the reading process. For such a case, Eq. (8) is still valid, and the material parameter space is again given by Fig. 2. instead of Fig. 3, in which η now is the efficiency of the photon-gating process. For processing-type applications, all the atoms that are in the upper state after the data pulse sequence participate in the storage and

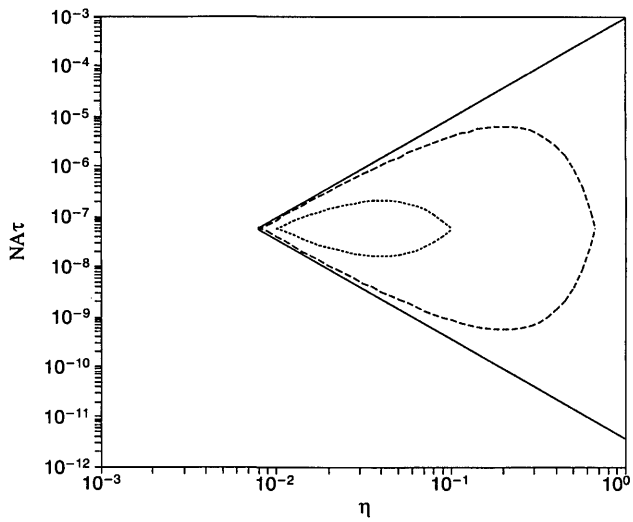

Fig. 3. Permitted material parameter space for time-domain optical storage with destructive reading. The storage density equals the theoretical limit for conventional optical storage. The numbers of consecutive readings are 1, 5, and 25 (solid, long-dashed, and short-dashed curves, respectively). The permitted area decreases as the number of reads increase. η and $NA\tau$ are the same as in Fig. 2.

processing operations. This corresponds to the case $\eta = 1$ in Fig. 2 and is consequently particularly favorable.

D. Thermal Restrictions on Time-Domain Optical Storage

In the derivation of inequalities (10) and (13) it was assumed that the electromagnetic field of each single data pulse E_d was sufficient to rotate the Bloch vector of the system an angle $\pi/(2N)$ [Eq. (5)]. (Any smaller value for the pulse area of the data pulses would decrease the permissible area in Figs. 2 and 3.) It is reasonable to demand that the data pulse intensity I necessary for obtaining this pulse area should be less than I_{th}, where I_{th} is the maximum intensity for which the laser-pulse-generated thermal energy that is dissipated in the sample can be removed by cooling without an increase in the sample temperature. Based on the arguments above, the following equations are obtained:

$$\frac{dE_d\tau}{\hbar} = \frac{\pi}{2N} \tag{15}$$

($\hbar = h/2\pi$, where h is Planck's constant) and

$$I < I_{\text{th}}. \tag{16}$$

d is the transition dipole moment, i.e.,[20]

$$d^2 = \frac{3\epsilon_0 h\lambda^3}{16\pi^3} A. \tag{17}$$

Combined with

$$I = \tfrac{1}{2}c\epsilon_0 E_d{}^2 \tag{18}$$

(where ϵ_0 is the dielectric constant of vacuum and c is the speed of light), Eqs. (15) and (17) and inequality (16) yield

$$NA\tau > \pi\left(\frac{\pi}{6}\right)^{1/2}\left(\frac{hc}{\lambda^3}\right)^{1/2}\left(\frac{A}{I_{\text{th}}}\right)^{1/2}. \tag{19}$$

Below the limit for the value of $NA\tau$ given in inequality (19), it is no longer possible to cool the sample when data are continuously written and read from the sample. There has not been much discussion on how to choose I_{th} in this type of application. A typical value in optical computing is 100 W/cm^2 (Ref. 24). In the discussion section in Ref. 10 an intensity corresponding to 10^4 W/cm^2 is suggested for FDOS materials submerged in liquid helium at temperatures below the lambda point. Inequalities (10), (13), and (19) constitute a quite general restriction for TDOS materials. Inequality (19) is plotted in Fig. 4 for I_{th} equals 100 W/cm^2 and 10^4 W/cm^2.

3. Material-Dependent Restrictions on Time-Domain Optical Storage

So far, the graphs in this paper have been valued for stimulated photon echoes assuming storage material. As soon as one settles for a specific storage material the restrictions can be made more specific and new restrictions can also be defined. This is discussed below.

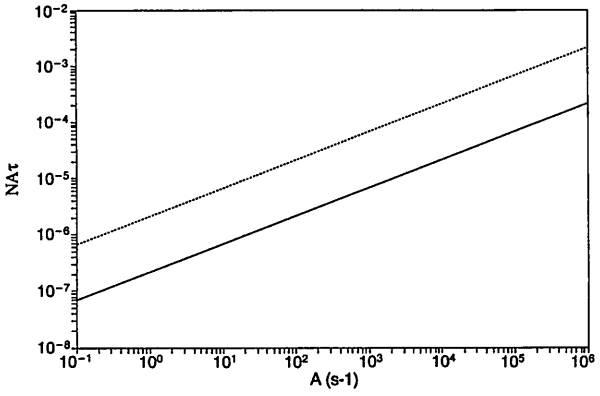

Fig. 4. Thermal considerations set a lower limit for the product $NA\tau$ (defined in Figs. 2 and 3) as a function of transition probability A. This lower limit is plotted assuming the highest laser intensity permitted is $I_{\max}$ = 100 W/cm^2 (dashed line) and $I_{\max}$ = 10,000 W/cm^2 (solid line), respectively.

A. Signal-to-Noise Ratio

Inequality (9) was analyzed by use of optimized material parameters. More generally, inequality (9) can be rewritten as an upper constraint on τ:

$$\tau < \frac{3\pi^2}{64}\frac{\xi}{\sqrt{\epsilon}} n_{\max}^2 \lambda^6 \eta^2 \frac{T^2}{S}\frac{AN}{(N/k^2)^3}. \tag{20}$$

If A is so small that $n_{\max}\sigma L < 0.3$, then inequality (20) is a more restrictive condition on τ than

$$\tau < \frac{27\pi^3}{1600 \ln 2}\frac{\xi}{\sqrt{\epsilon}}\eta^2 \frac{1}{SN}\frac{1}{A}\frac{1}{(N/k^2)}, \tag{21}$$

which is inequality (13) rewritten with $n\sigma L = 0.3$.

B. Relaxation

A lower limit on τ is, of course,

$$\tau > T. \tag{22}$$

This ascertains that the information can be stored within the inhomogeneous bandwidth. An additional higher limit is

$$\tau < \frac{T_2}{2N}. \tag{23}$$

This limit ascertains that the N bits are written in a time less than the homogeneous dephasing time of the transition, T_2. Inequalities (19)–(23) determine the possible bit rate as a function of the number of bits stored in each single point (assuming nondestructive reading), and the storage density may be used as a parameter in inequalities (20) and (21).

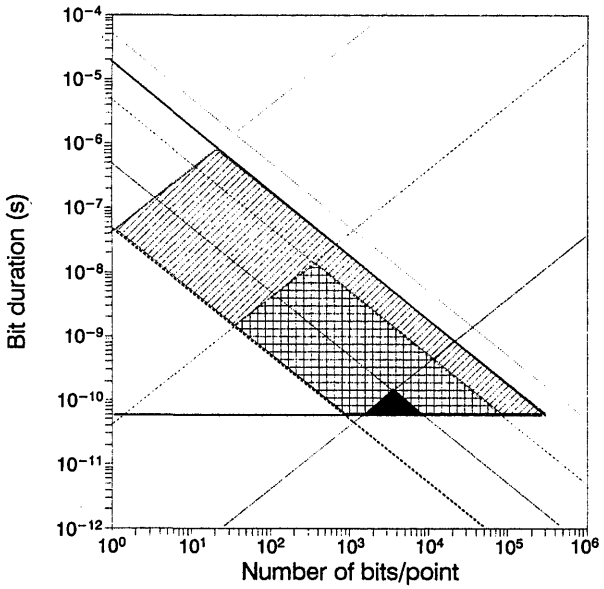

Fig. 5. Permitted values for the data bit duration versus the number of bits per point for optical processing with the $^3H_4$–$^1D_2$ transition in Pr:$YAlO_3$. Thick solid lines represent the following: the lower limit on bit duration (τ), set by the inhomogeneous bandwidth, and the upper limit on bit duration times the number of bits per point (τN), set by the homogeneous bandwidth. The thick dashed line is the thermal limit, giving a lowest value of τN. The three pairs of thin lines, the dotted, dashed, and solid ones, are SNR limits for storage densities (N/k^2) equal to 1, 10, and 100 times the theoretical limit for conventional optical storage, respectively. The SNR restrictions result in an upper limit on the bit duration. The permissible areas in (N, τ) space for the above three storage densities are shown as diagonally striped, cross-ruled, and filled-in areas, respectively.

C. Specific Example: $^3H_4$–$^1D_2$ Transition in Pr:$YAlO_3$

Specific values of several material parameters are necessary for a graphical display of the equations derived in Section 3. The $^3H_4$–$^1D_2$ transition in Pr:$YAlO_3$ is chosen to illustrate the calculations because the material parameters for this transition are relatively well known. Inequalities (19)–(23) are plotted in Fig. 5. The numerical values for the material parameters for the Pr:$YAlO_3$ $^3H_4$–$^1D_2$ transition are taken from Table 2 in Ref. 25 and they are as follows: transition probability, $A = 20\ s^{-1}$; inhomogeneous relaxation time, $T = 60$ ps; homogeneous relaxation time, $T_2 = 35\ \mu s$. The branching ratio η is calculated to be 6% from the theoretical estimates in Ref. 22. Since there currently appears to be no nondestructive reading process for this Pr transition, we chose to consider the data processing case $\eta = 1$ in Fig. 5. The relation between the different material parameters and the storage performance can still be discussed with no loss of generality. I_{th} in Eq. (19) was chosen to be $10^4\ W/cm^2$. The dark area is the permissible parameter space for storage densities greater than 100 times the conventional limit, the cross-ruled area is valid for densities that are more than ten times the limit, and the striped area is the permissible parameter space for a storage density better than the conventional limit. The thick horizontal line, independent of the number of bits addressed in a single point, represents inequality (22). An additional lower limit on τ is the thermal limit, inequality (19), which is the thick dashed line. The upper limits are inequality (23) (thick solid line) and the SNR limits, inequalities (20) and (21), for N/k^2 equal to 1, 10, and 100, which are represented by dotted, dashed, and thin solid lines, respectively.

4. Analysis of Results

The key result of the paper is presented in Fig. 2. Several things can be inferred from this figure. It shows that the highest storage density obtainable with photon-echo storage is approximately 100 times the theoretical storage density for conventional optical storage. It also shows that a high branching ratio for the writing process is necessary to achieve high storage densities. The maximum fractional increase in storage density compared with conventional optical storage N/k^2 is given in Table 3 for different branching ratios η. As another example of how Fig. 2 can give information on the material parameter requirements, assume that a readout time of 1 ns/bit is desired at a storage density of 100 times the conventional limit. As the branching ratio must be close to unity, it would be necessary to use a transition at which photon gating could be performed with an efficiency close to unity. (This would be the case unless the information should be read only one time and unless this would occur before the upper-state relaxation. In such a case there are no constraints on the branching ratio.) Next, assume that at this storage density $N/k^2 = 100$, we wish to address 1 kbit at each spatial point, with $N \cong 1000$. Because $NA\tau$ from Fig. 2 must equal 10^{-5}, the transition probability must equal $10\ s^{-1}$ for a bit rate of 1 GHz. For a given number of bits per point and a given storage density, the rate increases proportionally with the transition probability. This is also illustrated in Table 4. There, data rate $1/\tau$ versus transition probability A is shown, assuming a storage density of 10 times the conventional limit, 1000 bits/point, and 10% writing efficiency. Notably also, low transition probabilities give quite high rates. As $NA\tau$ from Fig. 2 must be a little less than 10^{-6} for the above values of N/k^2 and η, the thermal limit $I_{th} = 10^4\ W/cm^2$ in Fig. 4 yields a maximum value for the transition probability of $\sim 10/s$. Still another example is given in Table 5. Here the transition probability is chosen to be $1000\ s^{-1}$, and the data rate is given versus the number of bits per point, assuming

Table 3. Maximum Storage Density (N/k^2)[a] Versus Writing Efficiency (η)

η	N/k^2
0.008	1
0.08	10
0.8	100

[a]Fractional improvement in storage density in comparison with conventional optical storage.

Table 4. Data Rate versus Transition Probability[a]

Transition Probability A (s^{-1})	Data Rate $1/\tau$ (MHz)
0.001	1
0.01	10
0.1	100
1	1000
10	10000

[a]Thermal limit prevents higher transition probability A when $NA\tau = 10^{-6}$ (see Fig. 4). We assume that storage density is 10 times the conventional limit, that there are 1000 bits/point, and that writing efficiency is 0.1 (i.e., $N/k^2 = 10$, $N = 1000$, and $\eta = 0.1$).

unity writing efficiency and a 100-times fractional increase in storage density in comparison with conventional optical storage. As can be seen, the data rates can be very high, higher than terahertz levels, but it is also clear that this requires a material in which a truly large number of bits may be addressed in a single point.

From Fig. 3 it can essentially be concluded that, if the stored information should be read several times, nondestructive reading is a necessary condition for high-density TDOS storage. Figure 4 shows how thermal considerations affect the permissible material parameter space and complements Fig. 2 by restricting the values of $NA\tau$ as a function of A. It can be seen also that the weaker restriction on the permissible intensity in Fig. 4, $I_{th} = 10^4$ W/cm^2, reduces the permissible area in Fig. 2 to the upper half of the figure, unless strongly forbidden transitions, with $A < 0.1$ s^{-1}, are used. As an example of the information provided in Fig. 4, assume that writing can be performed by use of photon gating with an efficiency (branching ratio) of 10% and that N/k^2 should equal 10. From Fig. 2, $NA\tau$ must equal 10^{-6}, and from Fig. 4, we see then that if information is read and written continuously, the transition probability cannot be much larger than 10 s^{-1}. Thus the lower limit on the product $N\tau$ for this case is $10^{-6}/(10\ s^{-1}) = 10^{-7}$ s.

The limits in Figs. 2–4 are not valid for arbitrarily small values of A [compare the discussion of inequalities (20) and (21)]. When the parameters for the transition are known, the representation in Fig. 5 is more appropriate than that shown in Figs. 2 and 4. For a given material and transition the issue may be to select an appropriate combination of the parameters bit duration, bits per point, and storage density.

Table 5. Data Rate versus Bits per Point[a]

Number of Bits per Point N	Data Rate $1/\tau$ (GHz)
100	10
1000	100
10000	1000
100000	10000

[a]We assume that storage density is 100 times the conventional limit, that there is unity writing efficiency, and that the transition probability is 1000/s (i.e., $N/k^2 = 100$, $\eta = 1$, and $A = 1000$ s^{-1}).

From Fig. 5 it can be seen that a larger number of bits per point requires shorter bit duration to maintain the SNR. Equation (15) shows that the required laser field is unchanged by changes in N or τ as long as the product $N\tau$ is kept constant, because a larger number of bits per point means a larger area is required (at fixed storage density), the laser power for maintaining this electric field increases. The maximum requirement on the laser power is most easily calculated by multiplication of I_{th} by the storage area, which is calculated from the storage density and the number of bits per point. For example, $I_{th} = 10$ kW/cm^2, $N/k^2 = 10$, and 1000 bits/point yield a laser power of 5 mW at $\lambda = 700$ nm. The lower limit on the bit duration in Fig. 5 is set by the inhomogeneous relaxation time. For high storage densities the upper limit is set by the SNR from inequalities (20) and (21). For a storage density 100 times the conventional limit the SNR can be sufficient only if a large number of bits (several thousand) are stored in each point and if the reading speed is ~10 GHz.

It is of special interest to find as large a permissible area in (N, τ) space as possible for any specified storage density. As an aid for understanding how the permissible area is affected by the relevant material parameters, inequalities (19)–(23) are again plotted in Fig. 6 for a storage density of 10 times the conventional limit ($N/k^2 = 10$). The permissible area is the diagonally striped region. It is indicated how the different borders move as transition probability A, inhomogeneous dephasing time T, and homogeneous dephasing time T_2 changes. To understand

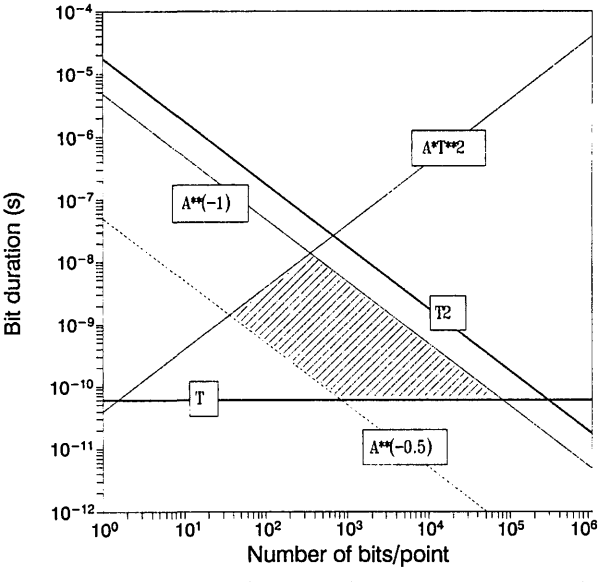

Fig. 6. Same thermal and bandwidth limits as in Fig. 5 are shown together with the SNR limits for a storage density equal to ten times the conventional limit. The permissible area in bit duration versus bits per point space is shown as a diagonally striped area. For each limit the dependence on the transition probability, A, the inhomogeneous dephasing time, T, and the homogeneous dephasing time, T_2, is shown. Thus the figure shows how the permissible area changes if these parameters change from their Pr $^3H_4$–$^1D_2$ transition values.

how the figure should be interpreted, consider the thermal limit. On this limit, $A^{-0.5}$ is written. This means that the thermal limit is independent of the homogeneous and inhomogeneous dephasing times, but it is inversely proportional to the square root of the transition probability. Increasing the transition probability by a factor of 4 therefore moves the thermal limit downward in the diagram by a factor of 2. This change in A also causes the SNR limit with negative slope [inequality (21)] to move downward by a factor of 4 and the SNR limit with positive slope [inequality (20)] to move a factor of 4 upward. To increase the bit rate, we must decrease the inhomogeneous dephasing time T. As can be seen from the permissible area, this also increases the number of bits that can be stored per spatial location. Decreasing the inhomogeneous phasing time, however, also rapidly lowers the SNR limit with the positive slope [inequality (20)]. It is clear from the figure that there is no general way to increase the permissible area infinitely, but by appropriate selection of transition probability and dephasing times the permissible area can generally be moved to any desired location in the diagram of bit duration versus bits per point.

5. Discussion

Our analysis is valid only for optically thin samples. Optically thick samples have the disadvantage of larger absorption, but the optimum performance of FDOS has been obtained at optical densities larger than 0.3, which we considered to be upper limit for the validity of our analysis. The case of high optical density is more complicated in TDOS than in FDOS because pulse propagation effects such as self-induced transparency strongly affect the physical description of photon echoes. Previous investigations of photon echoes in optically dense media (e.g., Refs. 26 and 27) imply that TDOS could perform better in more dense samples; however, from the analyses in Refs. 26 and 27 there is no indication that the improvement would be more than an order of magnitude. Therefore the limits calculated in this paper may be expected to be at least approximately valid for optically dense samples also.

It is at first sight surprising that SNR considerations, starting from only one expression [inequality (9)] can give both upper and lower limits on the material parameter space. For example, one could expect the SNR to always increase with increasing transition probability. The reason that the increase in SNR versus transition probability A is changed to a decrease for sufficiently large values of A is that the sample begins to absorb too large a fraction of the radiation (including the signal). If the goal were optimization of the volume storage density and not of the area storage density, too large an absorption with increased transition probability could be compensated for just by a decrease in the sample length. However, in this paper (as in similar investigations on FDOS[10,11]) the area storage density is optimized, and as the length (again as in previous studies[10,11]) is chosen in terms of the Rayleigh length, it is tied to the storage area and thus cannot be changed independently. Similarly it can be surprising that the SNR limits in Fig. 5 demand short bit duration for high storage densities. Intuitively one would expect the SNR to increase with bit duration. The reason that this is not the case can be seen in Eq. (2). The pulses are assumed to be Fourier limited, and since it is implicitly assumed in the model that the laser intensity is increased such that the pulse area is unchanged when the pulse is shortened, the number of atoms that are affected by the excitation pulse is inversely proportional to the bit duration. Consequently, shortening the pulse effectively means increasing the number of excited centers.

It is clear from Subsection 2.C that multiple reads with destructive reading are basically impossible for TDOS. Further, for high storage densities to be obtained, the branching ratio during writing of the information must be high, $>10\%$. In Ref. 11 it is pointed out that the branching ratios for FDOS materials so far have always been smaller than 1%. In the few TDOS materials tested so far, it can often be higher, e.g., the branching ratio for Pr:$YAlO_3$ ($^3H_4$–$^1D_2$ transition) is calculated to be 6% from the theoretical estimates in Ref. 22. Nevertheless, our results imply that unless accumulated photon echoes are employed, highly efficient photon gating is necessary in TDOS. As few materials have been investigated for TDOS, the abundance of materials with appropriate photon-gating efficiency is unknown. Finding such materials is therefore an interesting task for the future. There is certainly a large number of various types of TDOS measurements in which the restrictions derived must be adjusted. Specifically, several cases of slow writing processes, often of the order of several seconds, but with high readout rates (faster than terahertz levels for some cases) and excellent SNR's, have been demonstrated.[3–6] Our analysis assumes that both the writing and the reading processes have duration's shorter than the homogeneous relaxation time (while the storage time, of course, may be arbitrary). The analysis here is therefore more relevant for the approach in, e.g., Refs. 2, 7, 18, 28, and 29.

6. Summary

The first in-depth analysis to our knowledge of the potential performance of photon-echo storage has been presented, and some aspects on photon-echo data processing have also been considered. Quantitative predictions of speed and storage density have been derived from a signal-to-noise-ratio analysis based on the number of photons in the photon-echo data output signal. The influences of different material parameters (e.g., transition probability, dephasing times, and branching ratios in the excited-state decay process) on the storage density, the number of bits per point, and the reading and writing speed, have been assessed. For any specified data storage or processing requirements the analysis should also

be helpful for understanding which material parameters to pay attention to and what their optimum values would be in order to fulfill the required performance.

The support by S. Svanberg and M. Aldén is gratefully acknowledged. This work was funded by the Swedish Natural Research Council and the Research Council at the Swedish Board for Technical Developments.

Note added in proof: It has recently been theoretically analyzed[30] and experimentally shown[31] that so-called coherent saturation can be removed by biphase coding the data sequence. The effect of this is that the condition in Eq. (5), $\theta_d = \pi/(2N)$, can be relaxed, and θ_d may approach the limit $\theta_d = \pi/[2(N)]$, which may increase the theoretical storage density significantly, more than an order of magnitude, for large N.

References

1. T. W. Mossberg, "Time-domain frequency-selective optical data storage," Opt. Lett. **7,** 77–79 (1982).
2. Y. S. Bai, W. R. Babbitt, N. W. Carlson, and T. W. Mossberg, "Real-time optical waveform convolver/cross correlator," Appl. Phys. Lett. **45,** 714–716 (1984).
3. S. Saikan, T. Kishida, A. Imaoka, K. Uchikawa, A. Furusawa, and H. Oosawa, "Optical memory based on heterodyne-detected accumulated photon echoes," Opt. Lett. **14,** 841–843 (1989).
4. M. Mitsunaga and N. Uesugi, "248-bit optical data storage in Eu^{3+}:$YAlO_3$ by accumulated photon echoes," Opt. Lett. **15,** 195–197 (1990).
5. V. L. da Silva, Y. Silberberg, J. P. Heritage, E. W. Chase, M. A. Saifi, and M. J. Andrejco, "Femtosecond accumulated photon echo in Er-doped fibers," Opt. Lett. **16,** 1340–1342 (1991).
6. A. Débarre, J.-C. Keller, J.-L. Le Gouët, P. Tchénio, and J.-P. Galaup, "Optical information storage in condensed matter with stochastic excitation," J. Opt. Soc. Am. B **8,** 2529–2536 (1991).
7. S. Kröll, L. E. Jusinski, and R. Kachru, "Frequency-chirped copropagating multiple-bit stimulated echo storage and retrieval in Pr^{3+}:$YAlO_3$," Opt. Lett. **16,** 517–519 (1991).
8. *Persistent Spectral Hole Burning: Science and Application,* Vol. 16 of 1991 OSA Technical Digest Series (Optical Society of America, Washington, D.C., 1991).
9. W. E. Moerner, *Persistent Spectral Hole-Burning: Science and Applications* (Springer, New York, 1988), Chap. 7, pp. 251–307.
10. W. E. Moerner and M. D. Levenson, "Can single-photon processes provide useful materials for frequency-domain optical storage," J. Opt. Soc. B **2,** 915–924 (1985).
11. N. Murase, K. Horie, M. Terao, and M. Ojima, "Theoretical study of the recording density limit of photochemical hole-burning memory," J. Opt. Soc. Am. B **9,** 998–1005 (1992).
12. M. Mitsunaga, R. Yano, and N. Uesugi, "Time- and frequency-domain hybrid optical memory: 1.6-kbit data storage in Eu^{3+}:Y_2SiO_5," Opt. Lett. **16,** 1890–1892 (1991).
13. T. W. Mossberg, "Swept-carrier time-domain optical memory," Opt. Lett. **17,** 535–537 (1992).
14. S. Saikan, K. Uchikawa, and H. Ohsawa, "Phase-modulation technique for accumulated photon echo," Opt. Lett. **16,** 10–12 (1991).
15. X. A. Shen, Y. S. Bai, and R. Kachru, "Reprogrammable optical matched filter for biphase-coded pulse compression," Opt. Lett. **17,** 1079–1081 (1992).
16. I. D. Abella, A. Kurnit, and S. R. Hartmann, "Photon echoes," Phys. Rev. **141,** 391–406 (1966).
17. R. H. Dicke, "Coherence in spontaneous radiation processes," Phys. Rev. **93,** 99–110 (1954).
18. M.-K. Kim and R. Kachru, "Many-bit optical data storage using stimulated echoes," Appl. Opt. **28,** 2186–2189 (1989).
19. A. G. Andersson, R. L. Garwin, E. L. Hahn, J. W. Horton, G. L. Tucker, and R. M. Walker, "Spin echo serial storage memory," J. Appl. Phys. **26,** 1324–1338 (1955).
20. R. C. Hilborn, "Einstein coefficients, cross sections, f values, dipole moments, and all that," Am. J. Phys. **50,** 982–986 (1982).
21. A. C. G. Mitchell and M. W. Zeemansky, *Resonance Radiation and Excited Atoms* (Cambridge U. Press, Cambridge, 1971), Chap. 3, pp. 92–102.
22. L. E. Erickson, "Optical-pumping effects on Raman-heterodyne-detected multipulse rf nuclear-spin-echo decay," Phys. Rev. B **42,** 3789–3797 (1990).
23. A. Winnacker, R. M. Shelby, and R. M. Macfarlane, "Photon-gated hole burning: a new mechanism using two-step photoionization," Opt. Lett. **10,** 350–352 (1985).
24. B. E. A. Saleh and M. C. Teich, *Fundamentals of Photonics* Wiley, New York, 1991) p. 852.
25. R. M. Macfarlane and R. M. Shelby, "Coherent transient and hole-burning spectroscopy of rare earth ions in solids," in *Spectroscopy of Solids Containing Rare Earth Ions,* A. A. Kaplyanskii and R. M. Macfarlane, eds. (Elsevier, New York, 1987), p. 51.
26. E. L. Hahn, N. S. Shiren, and S. L. McCall, "Application of the area theorem to photon echoes," Phys. Lett. A **37,** 265–267 (1971).
27. R. Friedberg and S. R. Hartmann, "Superradiant damping and absorption," Phys. Lett. A **37,** 285–286 (1971).
28. X. A. Shen and R. Kachru, "High-speed pattern recognition by using stimulated echoes," Opt. Lett. **17,** 520–522 (1992).
29. D. Manganaris, P. Talagala, and M. K. Kim, "Spatial mixed binary multiplication by photon echoes," Appl. Opt. **31,** 2426–2429 (1992).
30. W. R. Babbitt, "Optical coherent transient memory systgems," in *Photonics for Processors, Neural Networks, and Memories,* J. L. Horner, B. Javidi, W. J. Micelli, and S. T. Kowell, eds. Proc. Soc. Photo-Opt. Instrum. Eng. **2026,** 2026–50 (1993).
31. Y. S. Bai and R. Kachru, "Coherent time-domain data storage with a spread spectrum generated by random biphase shifting," Opt. Lett. **18,** 1189–1191 (1993).